LETTER

doi:10.1038/nature10509

Inhibition of BET recruitment to chromatin as an effective treatment for MLL–fusion leukaemia

Mark A. Dawson[1,2]*, Rab K. Prinjha[3]*, Antje Dittmann[4]*, George Giotopoulos[1], Marcus Bantscheff[4], Wai-In Chan[1], Samuel C. Robson[2], Chun-wa Chung[5], Carsten Hopf[4], Mikhail M. Savitski[4], Carola Huthmacher[4], Emma Gudgin[1], Dave Lugo[3], Soren Beinke[3], Trevor D. Chapman[3], Emma J. Roberts[3], Peter E. Soden[3], Kurt R. Auger[6], Olivier Mirguet[7], Konstanze Doehner[8], Ruud Delwel[9], Alan K. Burnett[10], Phillip Jeffrey[3], Gerard Drewes[4], Kevin Lee[3], Brian J. P. Huntly[1]* & Tony Kouzarides[2]*

Recurrent chromosomal translocations involving the mixed lineage leukaemia (MLL) gene initiate aggressive forms of leukaemia, which are often refractory to conventional therapies[1]. Many MLL-fusion partners are members of the super elongation complex (SEC), a critical regulator of transcriptional elongation, suggesting that aberrant control of this process has an important role in leukaemia induction[2,3]. Here we use a global proteomic strategy to demonstrate that MLL fusions, as part of SEC[2,3] and the polymerase-associated factor complex (PAFc)[4,5], are associated with the BET family of acetyl-lysine recognizing, chromatin 'adaptor' proteins. These data provided the basis for therapeutic intervention in MLL-fusion leukaemia, via the displacement of the BET family of proteins from chromatin. We show that a novel small molecule inhibitor of the BET family, GSK1210151A (I-BET151), has profound efficacy against human and murine MLL-fusion leukaemic cell lines, through the induction of early cell cycle arrest and apoptosis. I-BET151 treatment in two human leukaemia cell lines with different MLL fusions alters the expression of a common set of genes whose function may account for these phenotypic changes. The mode of action of I-BET151 is, at least in part, due to the inhibition of transcription at key genes (*BCL2*, *C-MYC* and *CDK6)* through the displacement of BRD3/4, PAFc and SEC components from chromatin. *In vivo* studies indicate that I-BET151 has significant therapeutic value, providing survival benefit in two distinct mouse models of murine MLL–AF9 and human MLL–AF4 leukaemia. Finally, the efficacy of I-BET151 against human leukaemia stem cells is demonstrated, providing further evidence of its potent therapeutic potential. These findings establish the displacement of BET proteins from chromatin as a promising epigenetic therapy for these aggressive leukaemias.

Dysregulation of chromatin modifiers is a recurrent and sentinel event in oncogenesis[6]. Therapeutic strategies that selectively alter the recruitment and/or catalytic activity of these enzymes at chromatin therefore hold great promise as targeted therapies[6]. In this regard the bromodomain and extra terminal (BET) family of proteins (BRD2, BRD3, BRD4 and BRDT) provide an ideal 'druggable' target, because they share a common highly conserved tandem bromodomain at their amino terminus. Selective bromodomain inhibitors that disrupt the binding of BET proteins to histones have recently been described[7,8]; however, their true therapeutic scope remains untested.

To identify the nuclear complexes associated with ubiquitously expressed BETs (BRD2/3/4), we performed a systematic global proteomic survey. Specifically, this involved a tri-partite discovery approach (Fig. 1a). In the first approach, bead-immobilized analogues of I-BET762 (ref. 9) were incubated with HL60 nuclear extracts and bound proteins were analysed by quantitative mass spectrometry (Supplementary Table 1). This approach identified the BET isoforms and a large number of co-purifying proteins (Supplementary Tables 1 and 2), indicating that the BET isoforms reside in many distinct protein complexes. In the second approach, immunoprecipitation analyses with selective antibodies against BRD2/3/4 were performed (Supplementary Fig. 1 and Supplementary Tables 3 and 4). This was complemented with additional immunoprecipitations using selected antibodies against complex members ('baits') selected from the subset of proteins that were identified in the first approach (Fig. 1b right panel, Supplementary Fig. 2 and Supplementary Table 3). In the third approach, bead-immobilized histone H4(1–21; K5acK8acK12ac) acetylated peptides were used to purify protein complexes. These data were combined to highlight a list of complexes identified in all three methods (Fig. 1b left panel, Supplementary Fig. 3 and Supplementary Table 1). Finally, specificity of the I-BET762 and histone tail matrix was further assessed by competition experiments (Fig. 1c, Supplementary Figs 4, 5 and Supplementary Table 2). This strategy enabled the direct determination of the targets of the inhibitor, and the proteins associated with the target, with subunits of protein complexes exhibiting closely matching half-maximum inhibitory concentration (IC_{50}) values[10]. Taken together these stringent and complementary approaches provide a high confidence global data set encompassing all known[11–13] and several novel BET protein complexes (Fig. 1b and Supplementary Fig. 3). Among the novel complexes, we observed a prominent enrichment and dose-dependent inhibition of several components of the PAFc[4,5] and SEC[2,3] (Fig. 1b, c), which were confirmed by reciprocal immunoprecipitations in HL60 cells (Fig. 1b). Moreover, reciprocal immunoprecipitations in two MLL-fusion leukaemia cell lines (MV4;11 and RS4;11) confirmed the relationship of SEC with BRD4 in different cellular contexts (Fig. 1d). Together these data indicate that BRD3 and BRD4 associate with the PAFc and SEC and may function to recruit these complexes to chromatin. Given that these complexes are crucial for malignant transformation by MLL fusions[2–5] we tested the hypothesis that displacement of BET proteins from chromatin may have a therapeutic role in these leukaemias.

To progress our studies with an optimized therapeutic agent we developed I-BET151 (Fig. 1e); a novel dimethylisoxazole template, previously undisclosed as a BET bromodomain inhibitor. It was identified and optimized to retain excellent BET target potency (Fig. 1i) and selectivity (Fig. 1h, Supplementary Figs 5–10 and Supplementary Table 5) while enhancing the *in vivo* pharmacokinetics and terminal half-life to enable prolonged *in vivo* studies (Fig. 4a and Supplementary

[1]Department of Haematology, Cambridge Institute for Medical Research and Addenbrookes Hospital, University of Cambridge, Cambridge CB2 0XY, UK. [2]Gurdon Institute and Department of Pathology, Tennis Court Road, Cambridge CB2 1QN, UK. [3]Epinova DPU, Immuno-Inflammation Centre of Excellence for Drug Discovery, GlaxoSmithKline, Medicines Research Centre, Gunnels Wood Road, Stevenage SG1 2NY, UK. [4]Cellzome AG Meyerhofstrasse 1, 69117 Heidelberg, Germany. [5]Molecular Discovery Research, GlaxoSmithKline R&D, Stevenage SG1 2NY, UK. [6]Cancer Epigenetics DPU, Oncology R&D, GlaxoSmithKline, 1250 South Collegeville Road, Collegeville, Pennsylvania 19426, USA. [7]Lipid Metabolism Discovery Performance Unit, GSK R&D, 91951 Les Ulis Cedex, France. [8]University Hospital of Ulm Internal Medicine III Albert- Einstein-Allee 23, 89081 Ulm, Germany. [9]Department of Hematology, Erasmus University Medical Center, 3015 GE Rotterdam, The Netherlands. [10]Department of Hematology, Cardiff University School of Medicine, Cardiff, CF14 4XN, UK.

*These authors contributed equally to this work.

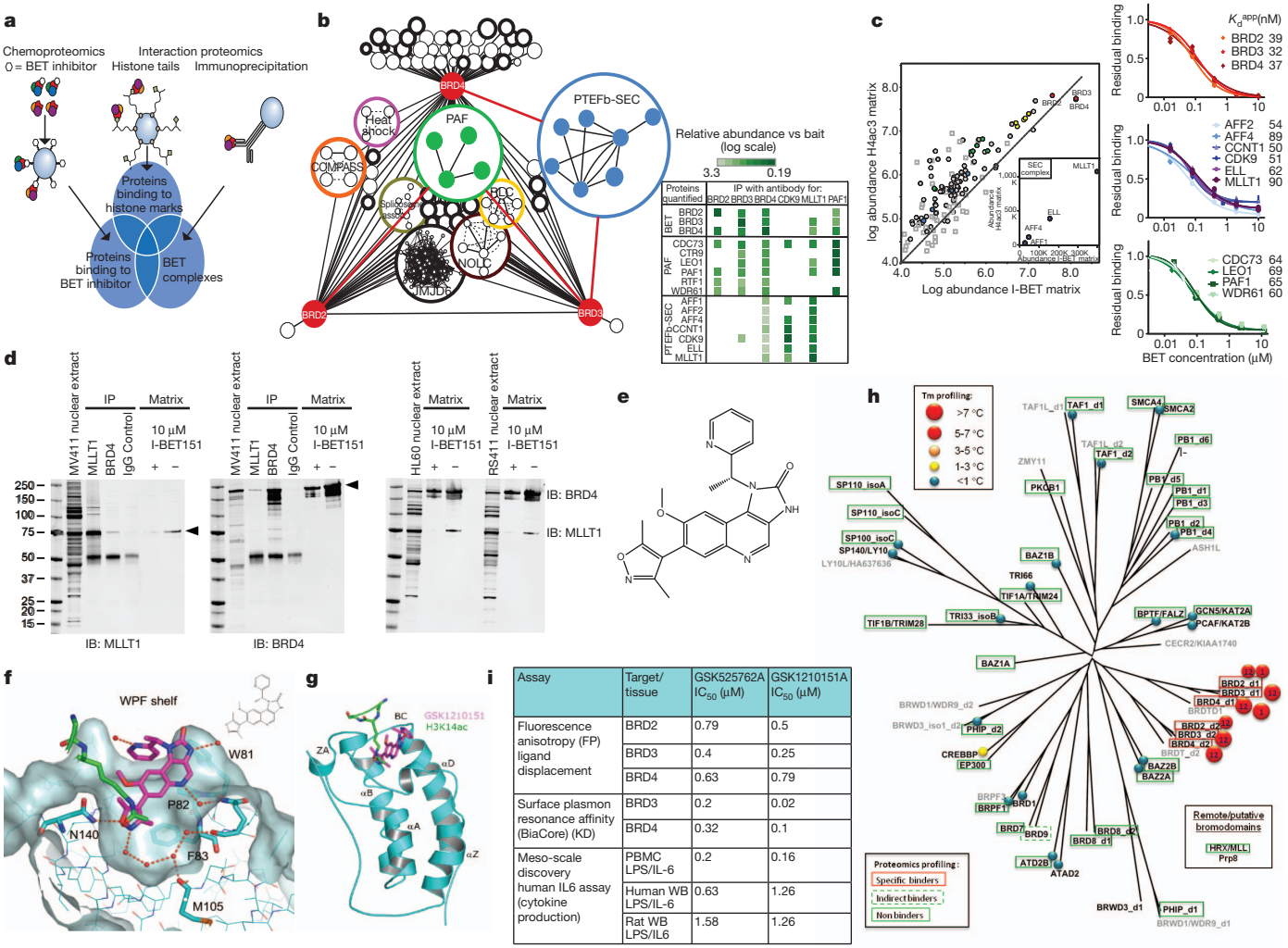

i

Assay	Target/ tissue	GSK525762A IC_{50} (μM)	GSK1210151A IC_{50} (μM)
Fluorescence anisotropy (FP) ligand displacement	BRD2	0.79	0.5
	BRD3	0.4	0.25
	BRD4	0.63	0.79
Surface plasmon resonance affinity (BiaCore) (KD)	BRD3	0.2	0.02
	BRD4	0.32	0.1
Meso-scale discovery human IL6 assay (cytokine production)	PBMC LPS/IL-6	0.2	0.16
	Human WB LPS/IL-6	0.63	1.26
	Rat WB LPS/IL6	1.58	1.26

Figure 1 | A global proteomic survey identifies BET proteins as part of the PAFc and SEC. **a**, Proteomic strategy. **b**, Left, Cytoscape representation of the BET protein complex network (discussed in detail in Supplementary Fig. 3). Bold circles indicate associations confirmed by the three orthogonal methods. Right, heat map representing quantitative-mass spectrometry data following co-immunoprecipitation of BETs, PAF and SEC complex members. **c**, Differential proteomic analysis of the proteins interacting with I-BET and triple acetylated histone H4 tail. Left, affinity matrices with immobilized I-BET762 or histone H4(K5acK8acK12ac) peptide bind to the same set of BET complexes. Protein abundance was determined from signal intensities in the mass spectrometer (arbitrary units, K = ×1,000). Right, competitive inhibition of the binding of BET isoforms, and SEC and PAF complex components, to the I-BET762 matrix showing matching concentration dependence. **d**, BRD4 and MLLT1 interact in HL60, MV4;11 and RS4;11 cells and binding to the I-BET762 matrix is blocked by excess I-BET151. **e**, Chemical structure of GSK1210151A (I-BET151). **f**, I-BET151 binding to the acetyl-binding pocket of BRD4-BD1 (cyan) overlaid with H3K14-acetyl peptide (green) (Protein Database ID 3jvk). A surface representation of the BRD4-BD1 is shown with key recognition and the specificity WPF shelf identified. **g**, Ribbon representation of the BRD4-BD1 (cyan) crystal structure complexed with I-BET151 (shown in magenta stick format) overlaid with H3(12-19)K14ac peptide (green) taken from its complex with BRD4-BD1(PDB ID 3jvk). Secondary elements of the BRD4-BD1 structure have been highlighted. **h**, Selectivity profile of IBET-151 showing average temperature shifts (T_m) using a fluorescent thermal shift assay. Numbering inside the spheres indicates bromodomains assessed; for example, 12 signifies both bromodomains 1 and 2 have been assessed. Overlaid is the selectivity profile generated using a proteomic approach (shown as boxes around proteins, discussed in Supplementary Fig. 5). Where the bromodomains have been profiled by both thermal shift and proteomic approaches the agreement is excellent. Proteins not assessed by either technique are shown in grey. **i**, Comparison of I-BET762 and I-BET151 potency in ligand displacement assays, direct Biacore binding and lipopolysaccharide-stimulated IL-6 cytokine production from human peripheral blood mononuclear cells (PBMC) or whole blood (WB).

Fig. 20). We also generated proteomic selectivity profiles comparing I-BET151 with I-BET762 (Fig. 1h, Supplementary Fig. 5 and Supplementary Table 6). We bead-immobilized a combination of differentially acetylated histone tail peptides (Supplementary Table 7), which captured a total of 27 bromodomain proteins from HL60 nuclear extracts. Competition with excess I-BET151 or I-BET762 blocked the capture of BRD2, BRD3, BRD4, and BRD9 but had no effect on the 23 other bromodomain proteins including MLL. The inhibition of BRD9 is likely to be indirect as this protein forms a complex with BRD4 (Supplementary Table 3). Finally, a high-resolution (1.5 Å) crystal structure of I-BET151 bound to BRD4-bromodomain 1 (BD1) revealed binding to the acetylated-lysine (AcK) recognition pocket of the BET protein (Fig. 1f, g and Supplementary Fig. 10).

To assess the therapeutic efficacy and selectivity of I-BET151, we tested a panel of leukaemic cell lines harbouring a spectrum of distinct oncogenic drivers. These data demonstrated that I-BET151 has potent efficacy against cell lines harbouring different MLL-fusions (Fig. 2a and Supplementary Fig. 11). To extend these data we tested the clonogenic potential of human leukaemic cells grown in cytokine-supplemented methylcellulose containing dimethylsulphoxide (DMSO; vehicle) or I-BET151. Consistent with the profound effects in liquid culture, the colony-forming potential of MLL-fusion-driven

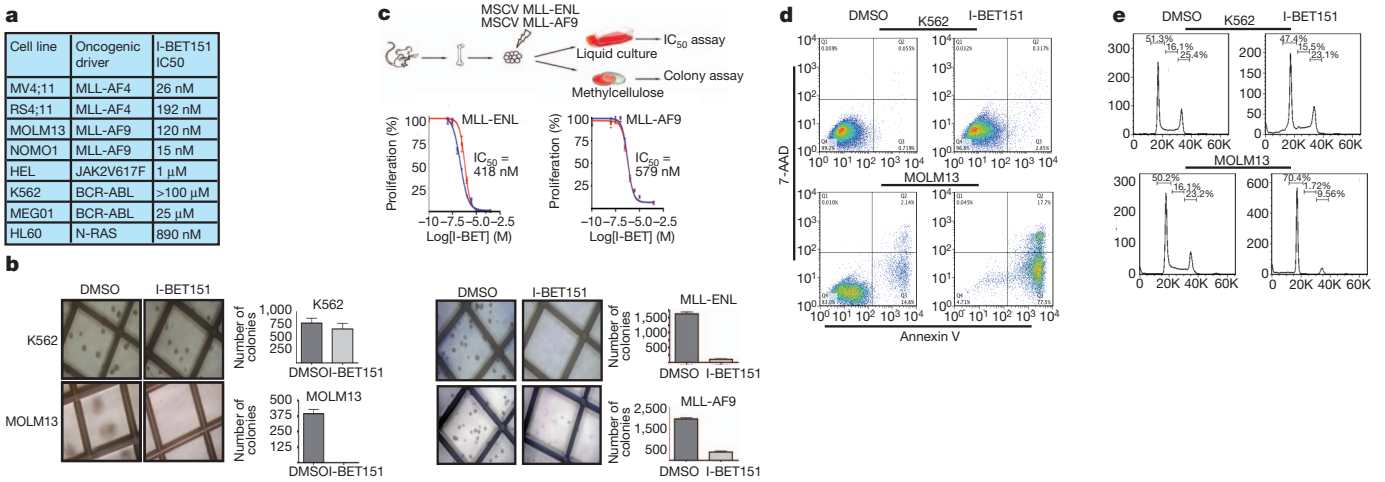

Figure 2 | I-BET151 selectively and potently inhibits MLL-fusion leukaemic cell lines *in vitro*. **a**, Human leukaemia cell lines tested using I-BET151. **b**, Clonogenic assays performed in the presence of DMSO or I-BET151. **c**, Haematopoietic progenitors were isolated from mouse bone marrow and retrovirally transformed with MLL–ENL or MLL–AF9. These cells were used in both proliferation and clonogenic assays **d**, Apoptosis was assessed by FACS analysis after 72 h incubation with DMSO or I-BET151. **e**, Cell cycle progression was assessed by FACS analysis 24 h after incubation with DMSO or I-BET151 (*y* axis event count, *x* axis arbitrary fluorescence units). Bar graphs are represented as the mean and error bars reflect standard deviation of results derived from triplicate experiments.

leukaemias (MOLM13) was completely ablated by I-BET151, whereas leukaemias driven by tyrosine kinase activation (K562) were unaffected (Fig. 2b). In addition to the data with human leukaemic cell lines, we also confirmed the potent efficacy of I-BET151 in both liquid culture and clonogenic assays using primary murine progenitors retrovirally transformed with either MLL-ENL or MLL–AF9 (Fig. 2c).

To investigate the mechanism of action for I-BET151, we performed fluorescence-activated cell sorting (FACS) analysis to assess apoptosis and cell cycle progression after I-BET151 treatment. Figure 2d–e and Supplementary Fig. 12 show a marked induction of apoptosis and a

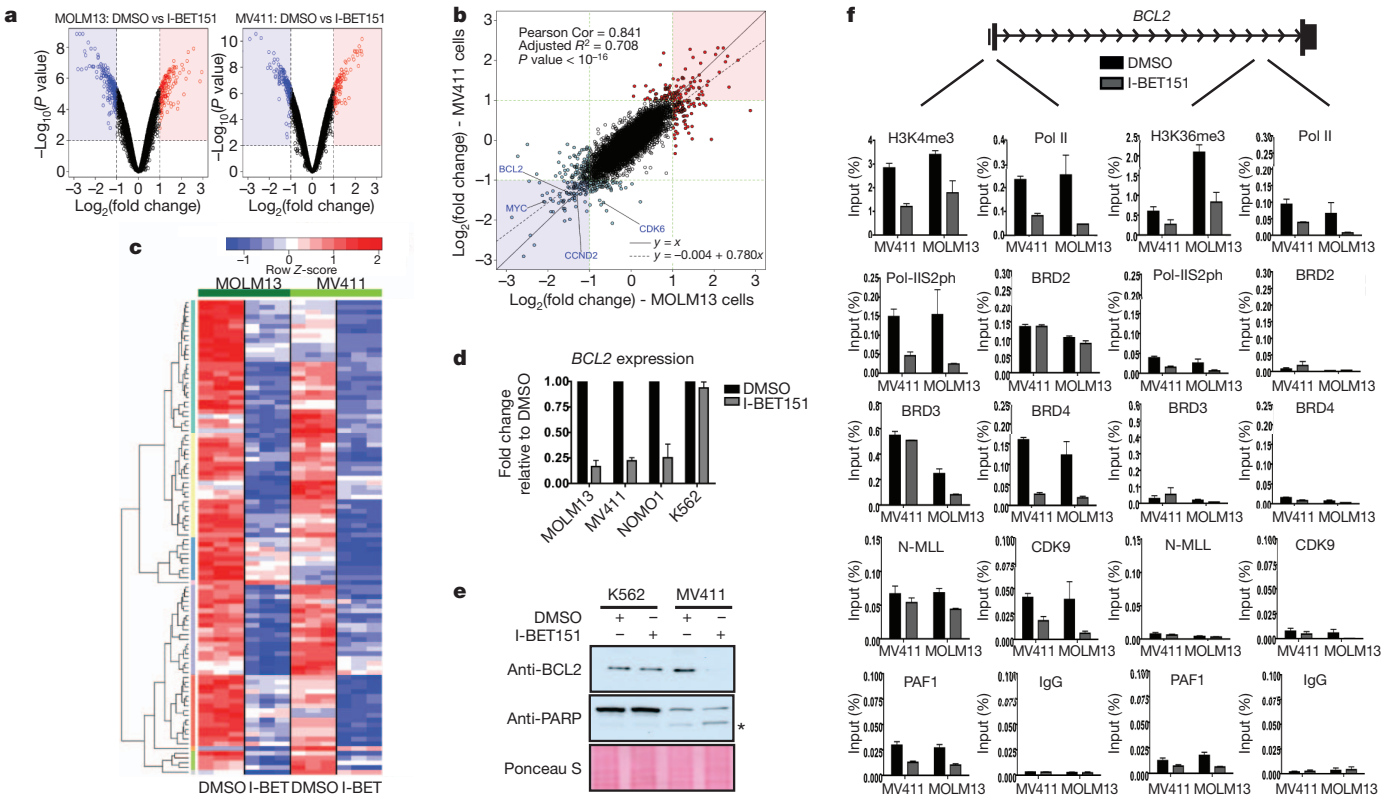

Figure 3 | Transcriptome and ChIP analyses provide mechanistic insights for the efficacy of I-BET151. **a**, Volcano plots for DMSO against I-BET151 treated samples, showing the adjusted significance *P* value ($\log_{10}$) versus fold change ($\log_2$). **b**, Correlation of $\log_2$ fold change between MV411 and MOLM131 across all genes. No genes show opposing expression changes. Lines represent the identity line (black solid), the line of best fit (black dotted), or $\log_2$ fold-change threshold values (green dotted). **c**, Heat map of top 100 genes downregulated following treatment with I-BET151. **d**, BCL2 gene expression (normalized to *B2M* expression) is shown. Expression level of *BCL2* in DMSO was assigned a value of 1. **e**, Immunoblotting demonstrating a decrease in BCL2 and an increase in cleaved PARP (*) after I-BET151 treatment. **f**, ChIP analysis at the TSS and 3′ end of *BCL2* is illustrated. Bar graphs are represented as the mean enrichment relative to input and error bars reflect standard deviation of results derived from biological triplicate experiments.

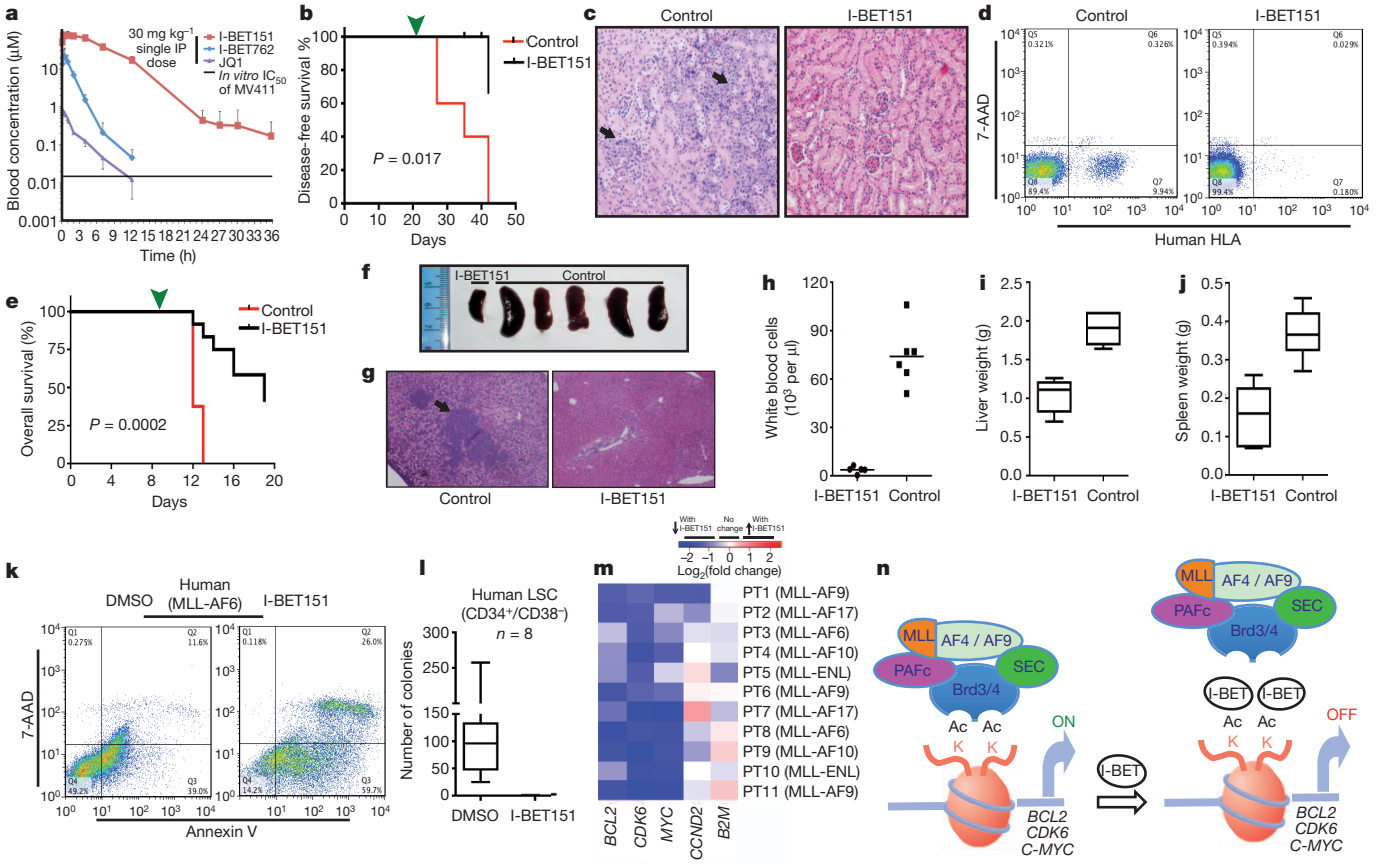

Figure 4 | I-BET151 is efficacious in *in vivo* murine models and primary patient samples of MLL-fusion leukaemia. **a**, Murine pharmacokinetic studies (mean ± s.d., $n = 4$ per compound) comparing the blood concentration of I-BET151 with I-BET762 and JQ1. **b**, Kaplan–Meier curve of control and treated NOD-SCID mice transplanted with 1×10^7 MV4;11 cells. Green arrowhead, treatment commencement on day 21. **c**, Haematoxylin and eosin-stained histological sections of the renal parenchyma of control and treated mice. Black arrows highlight leukaemic infiltration. **d**, Representative FACS analysis from the peripheral blood of control or I-BET151-treated mice. **e**, Kaplan–Meier curve of control and treated C57BL/6 mice transplanted with 2.5×10^6 syngeneic MLL–AF9 leukaemic cells. Green arrowhead, treatment commencement on day 9. **f**, Photomicrograph of the spleen size from 5/8 control and 1/12 I-BET151-treated mice that died on day 12. **g**, Haematoxylin and eosin-stained histological sections of the liver parenchyma from control and I-BET151-treated mice demonstrating reduced disease burden in the treated animal. **h–j**, Peripheral blood white cell count (**h**), liver weight (**i**) and spleen weights (**j**) from all the control and treated mice at the time of necropsy. **k**, Representative FACS analysis assessing apoptosis from a patient with MLL–AF6 leukaemia. **l**, Clonogenic assays with human MLL-fusion LSC isolated by FACS sorting ($CD34^+/CD38^-$) and plated in the presence of DMSO or I-BET151. **m**, Gene expression changes in human MLL-fusion leukaemia cells following treatment with I-BET151 or DMSO. The $\log_2$ fold change in the expression level for all genes (expression level with I-BET151 treatment/expression level with DMSO) is represented. **n**, Schematic model proposing the mode of action for I-BET151 in MLL-fusion leukaemia.

prominent G_0/G_1 arrest in two MLL-fusion cell lines driven by distinct MLL fusions (MOLM13 and MV4;11 containing MLL–AF9 and MLL–AF4, respectively). In contrast, the cell cycle characteristics and apoptotic rate of K562 cells were largely unaffected at this time. These data indicate that I-BET151 alters the transcriptional programmes regulating apoptosis and cell-cycle progression in MLL-fusion leukaemias.

To identify the precise transcriptional pathways controlled by I-BET151, global gene-expression analysis was performed in MOLM13 and MV4;11 cells after treatment with I-BET151 or DMSO for 6 h. This strategy allowed us to identify early I-BET151-responsive genes, before any discernable phenotypic alteration in cell cycle or apoptosis (Supplementary Fig. 12). As demonstrated previously[7], we observed differential expression of a selective subset of genes (Fig. 3a), rather than global transcriptional dysregulation. Remarkably, the transcriptional programmes altered in the two MLL-fusion cell lines were highly correlated (Fig. 3b) and gene set enrichment analysis documented significant overlap with published MLL fusion signatures including MLL-fusion leukaemia stem cells (LSC)[14,15] (Supplementary Fig. 13). These data are consistent with the notion that MLL fusions aberrantly co-opt the SEC and PAFc to regulate similar transcriptional programmes. Notably, the top 100 genes concomitantly decreased in both MOLM13 and MV4;11 (Fig. 3c) contained several previously reported direct MLL targets, such as *BCL2*, *CDK6* and *MYC*, the down-regulation of which was consistent with the phenotypic consequences of I-BET151 treatment.

BCL2 is a key antiapoptotic gene implicated in the pathogenesis of MLL-fusion leukaemias[16,17]. Consistent with these data, I-BET151 reduced the expression of *BCL2* in a third MLL-fusion cell line (NOMO1) but not in the unresponsive K562 cells (Fig. 3d), and induction of apoptosis coincided with a marked reduction in BCL2 protein expression (Fig. 3e). Moreover, overexpression of BCL2 in the presence of I-BET151 rescued the apoptotic phenotype (Supplementary Fig. 14). Chromatin immunoprecipitation (ChIP) analyses at the *BCL2* locus showed that 6 h of I-BET151 treatment selectively decreased the recruitment of BRD3/4 and impaired recruitment of CDK9 and PAF1 (part of SEC and PAFc, respectively) to the transcriptional start site (TSS). This correlated with reduced phosphorylation of RNA polymerase II (Pol II) on serine 2 of its carboxy-terminal domain (Pol-IIS2ph) (Fig. 3f). A similar pattern was observed at two other MLL target genes (*MYC* and *CDK6*), but not at housekeeping genes (*B2M*) whose expression was unaltered by I-BET151 (Supplementary Fig. 15).

Together, these data indicate that the mechanism of efficacy for I-BET151 involves a selective abrogation of BRD3/4 recruitment to chromatin. The consequence of this is the inefficient phosphorylation/recruitment of Pol II. Further investigation is necessary to distinguish whether Pol II recruitment and/or elongation is primarily affected by I-BET151.

We next sought to establish the therapeutic potential of I-BET151 *in vivo*. We first characterized the pharmacokinetic properties of I-BET151 in several preclinical species (Supplementary Fig. 20) and also compared it to published inhibitors[7,8] (Fig. 4a). We then assessed the efficacy of I-BET151 in two established models of MLL leukaemia. Our first model was a xenotransplant model of disseminated human MLL–AF4 leukaemia[18]. I-BET151 was delivered daily at 30 mg kg^{-1} by intraperitoneal injection from day 21 (ref. 18), and mice were humanely killed if clinical disease dictated or if there was a sequential rise in peripheral blood disease. At the experimental end-point all the control mice had succumbed to fulminant or progressive disease whereas only one out of five mice in the treated cohort had evidence of disease at low levels (Fig. 4b–d and Supplementary Fig. 16). In our second syngeneic model of murine MLL–AF9 leukaemia, 2.5×10^6 leukaemic cells, established from serial transplantation, were injected into tertiary recipients. Despite the latency being reduced to less than 15 days, we waited to initiate treatment from day 9 to test the efficacy of I-BET151 in the setting of overwhelming established disease (Fig. 4e), the scenario often encountered in clinical practice. Even here I-BET151 provided a clear and marked survival benefit (Fig. 4e–j and Supplementary Fig. 17). Taken together, these data demonstrate that I-BET151 provides excellent control of MLL leukaemia progression in two distinct and complementary murine models.

Finally, to demonstrate the applicability of our findings to human disease, we tested the efficacy of I-BET151 in leukaemia cells isolated from patients with various MLL fusions. These data show that I-BET151 accelerates apoptosis (Fig. 4k and Supplementary Fig. 18), and abrogates clonogenic efficiency in bulk leukaemia (Supplementary Fig. 19) as well as isolated LSC (Fig. 4l). These effects are driven, at least in part, by downregulation of a similar transcription programme identified in MLL-fusion cell lines (Fig. 4m). Taken together, these data provide compelling evidence of therapeutic potential and suggest that disease eradication is possible.

The paradigm for epigenetic drug discovery shown here highlights an emerging role for targeting aberrant transcriptional elongation in oncogenesis[2–5] and provides the first example in epigenetic therapy where mechanistic insights have driven targeted drug discovery and application (Fig. 4n). Together, our results suggest that perturbing the interaction of BET proteins with chromatin using I-BET151 may be of great therapeutic value in human MLL-fusion leukaemias. Using a complementary strategy and a different BET inhibitor, a separate study published in this issue concurs with this view[19]. Moreover, the extensive proteomic resource provided here has identified other important disease-associated proteins binding to BET proteins, such as MMSET (WHSC1), which is implicated in multiple myeloma[20]. This raises the possibility that BET inhibitors may have an even wider therapeutic scope in oncology and perhaps in other areas of unmet need within the clinical arena.

METHODS SUMMARY

Cell culture, gene expression, chromatin immunoprecipitation and FACS analysis were performed as previously described[21]. Proteomic profiling and characterization of inhibitor specificity was performed using methodology previously described[7,9,10]. Detailed information about the reagents and methodology used in this study is available in Supplementary Information.

Received 29 June; accepted 30 August 2011.

Published online 2 October; corrected 27 October 2011 (see full-text HTML version for details).

1. Krivtsov, A. V. & Armstrong, S. A. MLL translocations, histone modifications and leukaemia stem-cell development. *Nature Rev. Cancer* **7,** 823–833 (2007).
2. Lin, C. *et al.* AFF4, a component of the ELL/P-TEFb elongation complex and a shared subunit of MLL chimeras, can link transcription elongation to leukemia. *Mol. Cell* **37,** 429–437 (2010).
3. Yokoyama, A., Lin, M., Naresh, A., Kitabayashi, I. & Cleary, M. L. A higher-order complex containing AF4 and ENL family proteins with P-TEFb facilitates oncogenic and physiologic MLL-dependent transcription. *Cancer Cell* **17,** 198–212 (2010).
4. Milne, T. A. *et al.* Multiple interactions recruit MLL1 and MLL1 fusion proteins to the *HOXA9* locus in leukemogenesis. *Mol. Cell* **38,** 853–863 (2010).
5. Muntean, A. G. *et al.* The PAF complex synergizes with MLL fusion proteins at HOX loci to promote leukemogenesis. *Cancer Cell* **17,** 609–621 (2010).
6. Rodríguez-Paredes, M. & Esteller, M. Cancer epigenetics reaches mainstream oncology. *Nature Med.* **17,** 330–339 (2011).
7. Nicodeme, E. *et al.* Suppression of inflammation by a synthetic histone mimic. *Nature* **468,** 1119–1123 (2010).
8. Filippakopoulos, P. *et al.* Selective inhibition of BET bromodomains. *Nature* **468,** 1067–1073 (2010).
9. Chung, C. W. *et al.* Discovery and characterization of small molecule inhibitors of the BET family bromodomains. *J. Med. Chem.* **54,** 3827–3838 (2011).
10. Bantscheff, M. *et al.* Chemoproteomics profiling of HDAC inhibitors reveals selective targeting of HDAC complexes. *Nature Biotechnol.* **29,** 255–265 (2011).
11. Jang, M. K. *et al.* The bromodomain protein Brd4 is a positive regulatory component of P-TEFb and stimulates RNA polymerase II-dependent transcription. *Mol. Cell* **19,** 523–534 (2005).
12. Maruyama, T. *et al.* A mammalian bromodomain protein, Brd4, interacts with replication factor C and inhibits progression to S phase. *Mol. Cell. Biol.* **22,** 6509–6520 (2002).
13. Yang, Z. *et al.* Recruitment of P-TEFb for stimulation of transcriptional elongation by the bromodomain protein Brd4. *Mol. Cell* **19,** 535–545 (2005).
14. Somervaille, T. C. *et al.* Hierarchical maintenance of MLL myeloid leukemia stem cells employs a transcriptional program shared with embryonic rather than adult stem cells. *Cell Stem Cell* **4,** 129–140 (2009).
15. Wang, J. *et al.* Conditional MLL-CBP targets GMP and models therapy-related myeloproliferative disease. *EMBO J.* **24,** 368–381 (2005).
16. Robinson, B. W. *et al.* Abundant anti-apoptotic BCL-2 is a molecular target in leukaemias with t(4;11) translocation. *Br. J. Haematol.* **141,** 827–839 (2008).
17. Wang, Q. F. *et al.* MLL fusion proteins preferentially regulate a subset of wild-type MLL target genes in the leukemic genome. *Blood* **117,** 6895–6905 (2011).
18. O'Farrell, A. M. *et al.* SU11248 is a novel FLT3 tyrosine kinase inhibitor with potent activity *in vitro* and *in vivo*. *Blood* **101,** 3597–3605 (2003).
19. Zuber, J. *et al.* RNAi screen identifies Brd4 as a therapeutic target in acute myeloid leukaemia. *Nature* doi:10.1038/nature10334 (this issue).
20. Martinez-Garcia, E. *et al.* The MMSET histone methyl transferase switches global histone methylation and alters gene expression in t(4;14) multiple myeloma cells. *Blood* **117,** 211–220 (2011).
21. Dawson, M. A. *et al.* JAK2 phosphorylates histone H3Y41 and excludes HP1α from chromatin. *Nature* **461,** 819–822 (2009).

Supplementary Information is linked to the online version of the paper at www.nature.com/nature.

Acknowledgements We thank S. J. Dawson, A. Bannister, S. Anand and all members of the Huntly and Kouzarides laboratories. We are grateful to H. Doehner, the NCRI AML trials biobank and A. Giles for the provision of patient samples. We acknowledge D. Huang for the BCL2 expression plasmid, L. Gordon for supplying fluorescence resonance energy transfer data and R. Woodward, C. Delves, E. Jones and P. Holmes for protein production. J. Witherington, N. Parr, S. Baddeley and J. Seal provided compound selectivity data. We thank N. Deeks and L. Cutler for providing sample and PK data analysis. We acknowledge K. Smitheman and A. Wyce for help with the cellular analysis of the BET inhibitors, P. Grandi for suggestions and discussion, S. Chan for biophysical assay data, and members of the Epinova team for discussion and suggestions. We thank staff at the ESRF at Grenoble for beamline assistance. We thank T. Werner for assistance with mass spectrometry experiments and data analysis, and the members of the Cellzome Biochemistry, Mass Spectrometry, and IT teams for outstanding expertise and diligence. This work was supported by a Wellcome-Beit Intermediate Clinical Fellowship to M.A.D. The Huntly lab is funded by the Medical Research Council (UK), Leukaemia Lymphoma Research (UK), the Wellcome Trust, The Leukemia & Lymphoma Society of America, Cancer Research UK (CRUK) and the NIHR Cambridge Biomedical Research Centre. This work in the Kouzarides laboratory was funded by a programme grant from Cancer Research UK (CRUK).

Author Contributions M.A.D., R.K.P., A.D., G.D., K.L., P.J., B.J.P.H. and T.K. designed the research, interpreted data and wrote the manuscript. M.A.D., A.D., G.G., M.B., W.-I.C., S.C.R., C.-w.C., C.H., M.M.S., C.H., E.G., D.L., S.B., T.D.C., E.J.R., P.E.S., K.R.A. and O.M. performed experiments and analysed data. K.D., R.D. and A.K.B. provided patient samples. M.A.D., R.K.P. and A.D. are joint first authors.

Author Information Reprints and permissions information is available at www.nature.com/reprints. The authors declare no competing financial interests. Readers are welcome to comment on the online version of this article at www.nature.com/nature. I-BET151 compound requests should be directed to K.L. (kevin.2.lee@gsk.com). Correspondence and requests for materials should be addressed to B.J.P.H. (bjph2@cam.ac.uk), M.A.D. (mafd2@cam.ac.uk) or T.K. (t.kouzarides@gurdon.cam.ac.uk).